




Stochastic switches of eutrophication and oligotrophication: Modeling extreme weather via non-Gaussian Lévy noise

Cite as: Chaos 32, 043116 (2022); <https://doi.org/10.1063/5.0085560>

Submitted: 18 January 2022 • Accepted: 29 March 2022 • Published Online: 13 April 2022

 Anji Yang,  Hao Wang,  Tonghua Zhang, et al.



[View Online](#)



[Export Citation](#)



[CrossMark](#)

APL Machine Learning

Open, quality research for the networking communities

OPEN FOR SUBMISSIONS MAY 2022

[LEARN MORE](#)

AIP
Publishing

Stochastic switches of eutrophication and oligotrophication: Modeling extreme weather via non-Gaussian Lévy noise

Cite as: Chaos 32, 043116 (2022); doi: 10.1063/5.0085560

Submitted: 18 January 2022 · Accepted: 29 March 2022 ·

Published Online: 13 April 2022



View Online



Export Citation



CrossMark

Anji Yang,¹ Hao Wang,² Tonghua Zhang,³ and Sanling Yuan^{1,a)}

AFFILIATIONS

¹College of Science, University of Shanghai for Science and Technology, Shanghai 200093, China

²Department of Mathematical and Statistical Sciences, University of Alberta, Edmonton, Alberta T6G 2G1, Canada

³Department of Mathematics, Swinburne University of Technology, Hawthorn, Victoria 3122, Australia

^{a)}Author to whom correspondence should be addressed: sanling@usst.edu.cn

ABSTRACT

Disturbances related to extreme weather events, such as hurricanes, heavy precipitation events, and droughts, are important drivers of evolution processes of a shallow lake ecosystem. A non-Gaussian α -stable Lévy process is esteemed to be the most suitable model to describe such extreme events. This paper incorporates extreme weather via α -stable Lévy noise into a parameterized lake model for phosphorus dynamics. We obtain the stationary probability density function of phosphorus concentration and examine the pivotal roles of α -stable Lévy noise on phosphorus dynamics. The switches between the oligotrophic state and the eutrophic state can be induced by the noise intensity σ , skewness parameter β , or stability index α . We calculate the mean first passage time, also referred to as the mean switching time, from the oligotrophic state to the eutrophic state. We observe that the increased noise intensity, skewness parameter, or stability index makes the mean switching time shorter and thus accelerates the switching process and facilitates lake eutrophication. When the frequency of extreme weather events exceeds a critical value, the intensity of extreme events becomes the most key factor for promoting lake eutrophication. As an application, we analyze the available data of Lake Taihu (2014–2018) for monthly precipitation, phosphorus, and chlorophyll-a concentrations and quantify the linkage among them using the Lévy-stable distribution. This study provides a fundamental framework to uncover the impact of any extreme climate event on aquatic nutrient status.

Published under an exclusive license by AIP Publishing. <https://doi.org/10.1063/5.0085560>

It is predicted that the frequency and intensity of extreme weather events will continue to increase in the near future. Therefore, it is necessary to investigate the effects of extreme weather on nutrient dynamics in shallow lakes. In this paper, we argue that such a transition from the oligotrophic state to the eutrophic state could be triggered by extreme weather events. Thus, we extend the previous research to the framework of non-Gaussian α -stable Lévy noise, which can characterize unpredictable jump changes of the random environment. The environmental noise-induced switch behaviors have been investigated by considering the stationary probability density function of the phosphorus concentration. Furthermore, we characterize basic features of these transitions with simulations of stochastic tools (mean first passage time, MFPT). The results clearly indicate that the non-Gaussian α -stable Lévy noise can better cause the switches between different nutritional levels, and the switching process is

significantly accelerated compared with Gaussian noise. We also analyzed monthly precipitation, P concentration, and chlorophyll-a (Chl-a) concentration data of Lake Taihu (2014–2018) and quantify the linkage among them using the Lévy-stable distribution. This method is novel in describing the nutrient pulsing in shallow lakes by Lévy noise and can be widely applied to the quantitative description of sudden weather events in any ecological model.

I. INTRODUCTION

Lake Taihu is located in the Yangtze Delta, the most industrialized area in China with high population density, urbanization, and economic development.¹ It is the third largest freshwater lake in China and provides vital drinking water for roughly 10×10^6

residents in neighboring cities. In 2007, however, a serious drinking water crisis took place in Wuxi, Jiangsu Province, in China. About 2×10^6 residents had no water to drink for at least a week because of algal blooms that have gathered at drinking water intakes.² Increased evidence suggested that the primary cause of the crisis was the accumulation of nutrient-rich sewage and agricultural runoff in Lake Taihu, which contributed to severe eutrophication. Moreover, the abnormally hot and dry weather condition in early summer might be the culprit for the bloom during 2007.²⁻⁴

In general, in an oligotrophic lake, the nutrient concentration is mainly affected by inputs from the watershed, whereas in a eutrophic lake, it is controlled by recycling within the lake and inputs simultaneously.⁵ Some studies show that there are fluctuations in both the internal nutrient circulation process and the external nutrient input process of a lake.^{6,7} On the one hand, in a shallow lake, the process of nutrient recycling within the lake is easily disturbed by wind, which causes sediment resuspension and leads to the release of nutrients from the lake bottom.⁸ For example, S ndergaard *et al.*⁹ performed laboratory experiments to observe that the internal phosphorus loading induced by resuspension is estimated to be 20–30 times greater than the release from undisturbed sediments. On the other hand, nonpoint sources of nutrients, such as runoff from agricultural or urban lands, are also one of the pivotal factors driving lake eutrophication.¹⁰ Analyses of historical data show that major rainfall events can interact with manure and fertilizer in agricultural watersheds to increase erosion and nutrient transport to surface waters.¹¹ As a summary, extreme weather events such as heavy rains, typhoons, prolonged droughts, and extreme heat, which occur rarely, unforeseeable, and fiercely, can significantly impact the nutrient level in a lake. Therefore, it is necessary to investigate the effects of extreme weather on phosphorus dynamics in shallow lakes.

In a natural lake, the disturbance to the ecosystem caused by random factors such as extreme weather is inevitable. Extreme

weather events exacerbate physical, chemical, and biological disturbances in water columns.¹² In Fig. 1, we show the monthly chlorophyll-a biomass in Lake Taihu from 2005 to 2012. Solid green circles represent the biomass of chlorophyll-a in September of every year, and the names and dates of five typhoons passed Taihu are marked with arrows during these eight years. This figure illustrates that after each typhoon passage, the concentration of chlorophyll-a rises to a larger value. Table I shows the changes of phosphorus concentration in Lake Taihu before and after the typhoons passed. During the most severe algal bloom season of each year (August and September), phosphorus concentrations showed similar trends with chlorophyll-a. The pulses in nutrient status during extreme weather disturbances played a key role in the formation of algal blooms.

In the perspective of stochastic modeling methodology, Gaussian white noise is often used to describe the sum of low-intensity and independent random interference in the environment, whereas non-Gaussian noise often characterizes pulsing random interference with low frequency and large amplitude. Many studies in recent years have been devoted to exploring the effects of stochastic fluctuations on phosphorus concentrations under the Gaussian white noise framework. For instance, Ma *et al.*¹⁴ considered a parameterized lake eutrophication model with Gaussian white noise and periodic force and calculated the mean first passage time (MFPT) and the mean velocity (MV) of the first right-crossing process (from the oligotrophic state to the eutrophic state). In addition, their another work proposed two early warning indicators to predict noise-induced critical transitions for this lake eutrophication model under disturbance characterized by Gaussian white noise.¹⁵ Carpenter and Brock¹⁶ incorporated input noise and recycling noise into the deterministic model in Ref. 10, and numerical simulations showed that rising standard deviation could predict imminent critical transitions about a decade in advance. However, high-frequency data¹⁷ suggested that extreme weather conditions would cause heavy-tailed distribution of daily phosphorus loading. Therefore, in order to

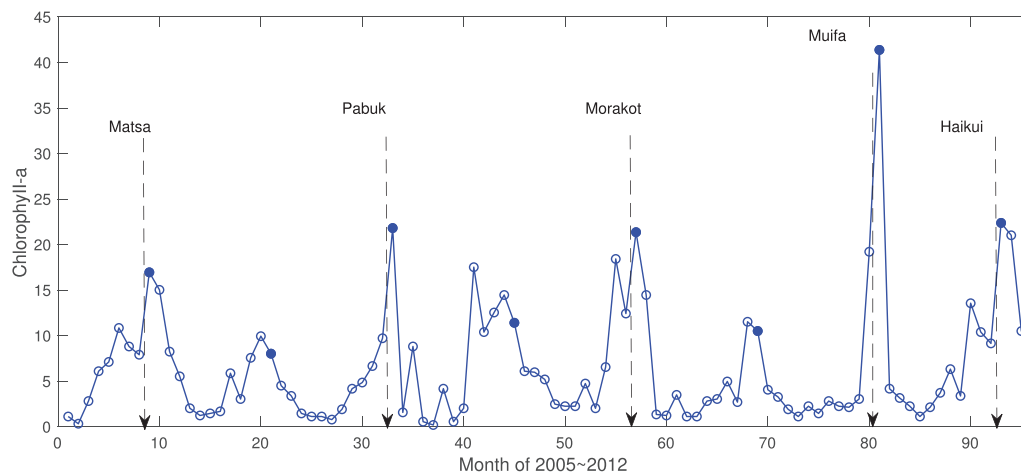


FIG. 1. Monthly chlorophyll-a biomass in Lake Taihu from 2005 to 2012. Solid green circles represent chlorophyll-a biomass in September of every year. Five typhoons that passed Lake Taihu are marked with names and dates by arrows.¹³

TABLE I. Phosphorus concentration in water of the entire lake before and after "August typhoon" from 2005 to 2012.¹³

Typhoons in August	Month	Total phosphorus (mg/l)
Haikui (2012)	August	0.171
	September	0.251
Muifa (2011)	August	0.256
	September	0.298
Morakot (2009)	August	0.115
	September	0.207
Pabuk (2007)	August	0.169
	September	0.209
Matsa (2005)	August	0.143
	September	0.152

simulate the burst-like events, non-Gaussian noise seems more suitable. We introduce α -stable Lévy process to model such non-Gaussian noise with unpredictable jumps and heavy tail. So far, Lévy noise has been frequently encountered in complex systems and applied in many other fields. For example, La Cognata *et al.*¹⁸ investigated a Lotka–Volterra competition model subject to α -stable Lévy noise and find quasi-periodic oscillations and a stochastic resonance phenomenon in the dynamics. Zhang *et al.*¹⁹ considered the transition behavior of the high vegetation biomass in the Grazing Ecosystem subject to Gaussian noise and Lévy noise, respectively. Chechkin *et al.*^{20,21} investigated the particle escape problem driven by Lévy noise and obtained the result in which the probability density function (PDF) of escape time decays exponentially. Moreover, there exist many interesting results on the Lévy noise-induced state transitions between domains of attraction of two deterministic attractors; one can see Refs. 22, 24 and the references therein for more details. However, to the best of our knowledge, no research has been done on the transition behavior of lake eutrophication via the method of non-Gaussian Lévy noise. Furthermore, nonlinear dynamical systems disturbed by noise can evoke unexpected events, which do not occur in the deterministic version, such as stochastic resonance,^{25,26} noise-induced state transitions,^{15,19,27} and noise-induced chaos.²⁸ Therefore, exploring the influence of external environmental disturbances on the evolution of phosphorus concentration is of great significance to clarify the dynamic mechanism behind the eutrophication of shallow lakes.

This paper mainly focuses on the switching behavior of a parameterized lake eutrophication model subject to α -stable Lévy noise and uncover the influence of Lévy noise parameters on the switching behavior. We organize the remaining sections of this paper as follows. In Sec. II, we first introduce the deterministic phosphorus dynamical model and α -stable Lévy distribution and then present the details of the stochastic phosphorus dynamical model driven by α -stable Lévy noise. Section III A provides our numerical method to simulate stochastic system (2) and examine the effects of Lévy noise parameters on phosphorus dynamics. In Sec. III B, we obtain the expected time that the solution of model (2) takes to switch from the low phosphorus state to the high phosphorus state. In Sec. III C, we analyze the real data of Lake Taihu and use the Lévy-stable distribution to quantify the relationship among extreme

monthly precipitation, Chl-a concentration, and P concentration. Finally, we conclude and discuss our results in Sec. IV.

II. METHODS AND MODELS

A. The deterministic model

This section is to introduce the deterministic lake eutrophication model developed by Carpenter *et al.*²⁹ describing the phosphorus dynamics in lakes. The model is defined as follows:

$$\frac{dP}{dt} = \underbrace{a}_{\text{input}} - \underbrace{bP}_{\text{loss}} + \underbrace{\frac{rP^q}{m^q + P^q}}_{\text{recycle}}. \quad (1)$$

The dynamic variable P is the phosphorus concentration in the lake water at time t . All parameters are positive, and a is the rate of phosphorus input from watershed. It is shown that the phosphorus input is a by-product of human activities such as agricultural production, forestry, and urban development. We assume that a is the control parameter. The loss caused by sedimentation and outflow is modeled by the linear term bP , where b is the phosphorus loss rate. In addition, phosphorus can be recycled from sediments or by consumers. The parameter r represents the maximum recycling rate. The exponent q describes the recycling relationship to phosphorus concentration. The phosphorus concentration at which recycling reaches half of the maximum rate is m . The major fluxes of phosphorus are charted in Fig. 2. In this paper, parameters in model (1) are taken as $b = 1$, $r = 1$, $m = 1$, and $q = 8$ as in Ref. 30. The bifurcation diagram of equilibria for deterministic model (1) with respect to the phosphorus loading rate a is shown in Fig. 3(a). For $a \in (0.2, 0.388]$, model (1) has only one equilibrium, corresponding to the oligotrophic state. For a given $a \in (0.388, 0.659)$ (in the tinted region), the system possesses two stable equilibria (the

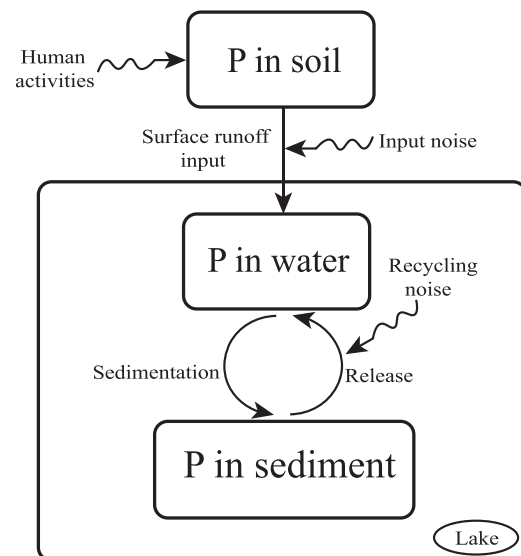


FIG. 2. Phosphorus flows in model (1).

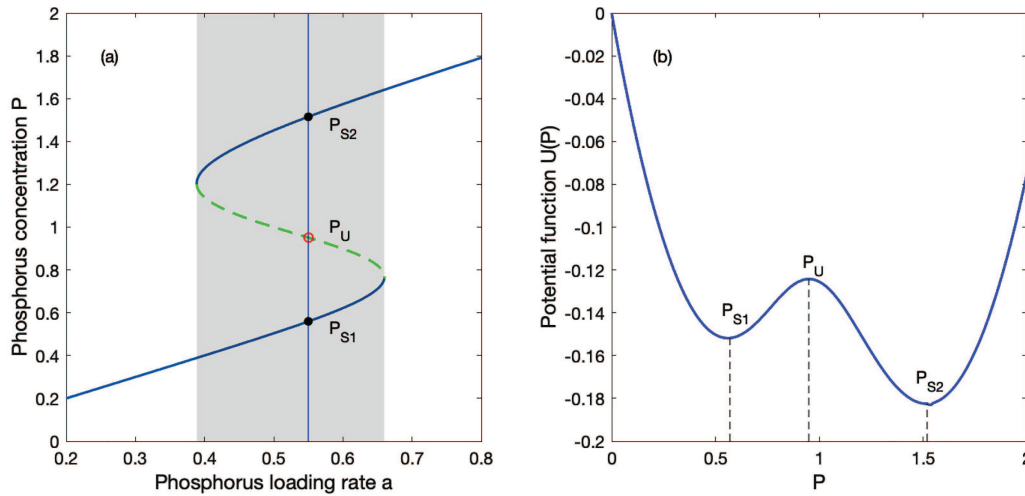


FIG. 3. (a) Bifurcation diagram for deterministic model (1) with respect to the loading rate a . The dashed curve represents the unstable equilibrium and solid curves represent the stable equilibria. (b) The potential function $U(P)$.

oligotrophic state P_{S1} and the eutrophic state P_{S2}) and one unstable equilibrium P_U . For $a \in [0.659, 0.8)$, there is only one stable equilibrium, which is the eutrophic state. In the deterministic phosphorus dynamical model, the evolution of model (1) relies on the choice of the initial phosphorus concentration. Only under the interference of a random environment, the switching behavior between the two nutritional states will occur. Therefore, we focus on the values of $a \in (0.388, 0.659)$ leading to bistability of model (1) and investigate how non-Gaussian Lévy noise affects the switching behavior. Here, we fix $a = 0.55$ to exhibit bistability and then the potential function $U(P)$ of the deterministic model (1) is shown in Fig. 3(b), whose local minima represent stable steady states of the phosphorus concentration.

B. The stochastic model

Both phosphorus recycling within the lake and nutrient input outside the lake are disturbed by environmental noise; thus, it is necessary to incorporate environmental noise into the deterministic model in an appropriate way. Figure 4 shows the time series of phosphorus concentration for different noise intensities. When the noise intensity is weak, the concentration of phosphorus fluctuates around the oligotrophic state. As the noise intensity increases, the stochastic trajectories escape from the attraction basin of the oligotrophic state into the attraction basin of the eutrophic state. Until the noise intensity increases to a certain threshold, the stochastic trajectories will frequently switch between the two attraction basins. Moreover, the switching time varies with the change of noise intensity. This switching mechanism is highly important for lake managers to prevent or mitigate an unwanted change; thus, it is meaningful to study the switching behaviors in phosphorus dynamics under environmental noise.

To investigate effects of stochastic fluctuations on the transitions between the oligotrophic and eutrophic regions, our stochastic

bistable model is described as

$$\frac{dP}{dt} = a - bP + \frac{rP^q}{m^q + P^q} + \frac{dL(t)}{dt}. \tag{2}$$

Here, $L(t)$ is a Lévy-stable motion with stationary and independent increments on non-overlapping time intervals. The process $L(t)$ is a generalized Wiener process obeying Lévy distribution $L(\zeta : \alpha, \beta, c, \mu)$. The formal time derivative of the Lévy process $L(t)$ denotes the Lévy noise, the general introduction of which is given in Ref. 31.

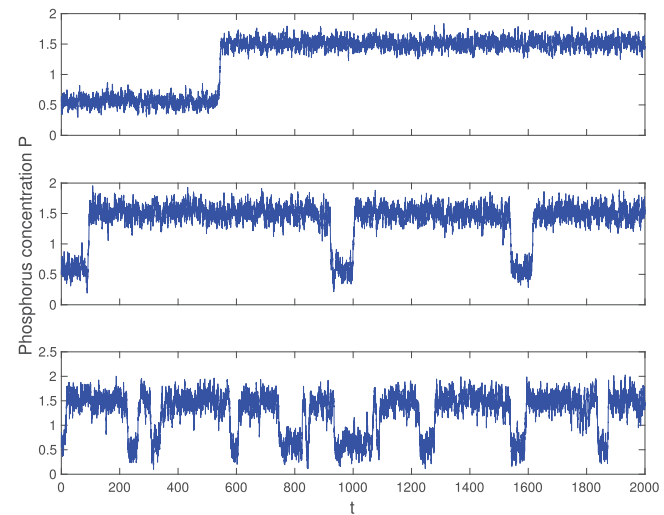


FIG. 4. Evolution of phosphorus concentration with initial status $P(0) = 0.55$ for $\alpha = 2$ and $\beta = 0$ at different noise intensities. From top to bottom, the intensity is $\sigma = 0.005$, $\sigma = 0.01$, and $\sigma = 0.02$.

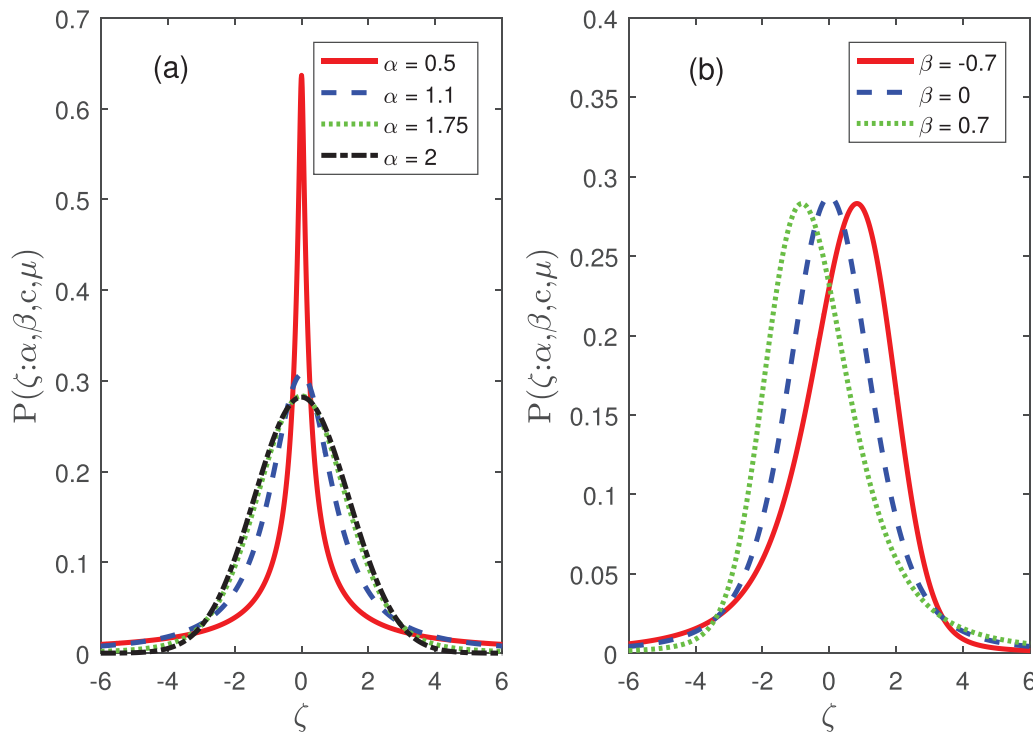


FIG. 5. (a) PDFs of $L(\zeta : \alpha, \beta, c, \mu)$ for different stability indices α ($\beta = 0, c = 1$, and $\mu = 0$); (b) PDFs of $L(\zeta : \alpha, \beta, c, \mu)$ for different skewness parameters β ($\alpha = 1.5, c = 1$, and $\mu = 0$).

The probability density function for a stable random variable is generally not representable via elementary functions. The most common and convenient way to introduce Lévy α -stable random variables is to define their characteristic function in the following form:^{32,33}

$$\varphi(\theta) = \begin{cases} \exp[-c^\alpha |\theta|^\alpha [1 - i\beta \operatorname{sgn}(\theta) \tan(\frac{\alpha\pi}{2}) + i\mu\theta]], & \alpha \neq 1, \\ \exp[-c|\theta| [1 + i\beta \operatorname{sgn}(\theta) \frac{2}{\pi} \ln|\theta| + i\mu\theta]], & \alpha = 1, \end{cases} \quad (3)$$

where parameter $\alpha \in (0, 2]$ is called the stability index, determining the thickness of the tail (the Gaussian distribution for $\alpha = 2$). The second parameter, which determines the skewness of the distribution, is designated β and lies in the range of $[-1, 1]$. The scale parameter c characterizes the deviation of the distribution, and $\sigma = c^\alpha$ is the noise intensity. μ acts as the location parameter that denotes the mean (or center) of the distribution.

Random variables ζ corresponding to the characteristic function (3) can be generated by the Chambers–Mallows–Stuck (CMS) algorithm³³ below:

For $\alpha \neq 1$,

$$X = A_{\alpha,\beta} \times \frac{\sin(\alpha(U + B_{\alpha,\beta}))}{(\cos(U))^{\frac{1}{\alpha}}} \times \left(\frac{\cos(U - \alpha(U + B_{\alpha,\beta}))}{V} \right)^{\frac{1-\alpha}{\alpha}}, \quad (4)$$

where

$$A_{\alpha,\beta} = \left[1 + \beta^2 \tan^2 \left(\frac{\alpha\pi}{2} \right) \right]^{\frac{1}{2\alpha}}, B_{\alpha,\beta} = \frac{\arctan(\beta \tan(\frac{\alpha\pi}{2}))}{\alpha}. \quad (5)$$

For $\alpha = 1$,

$$X = \frac{2}{\pi} \times \left[\left(\frac{\pi}{2} + \beta U \right) \tan(U) - \beta \log \left(\frac{\pi V \cos(U)}{2\beta U + \pi} \right) \right], \quad (6)$$

where U is uniformly distributed on $(-\frac{\pi}{2}, \frac{\pi}{2})$ and V is exponentially distributed with a unit mean, and U, V are independent random variables. We thus obtain the α -stable Lévy random variable

$$S = \begin{cases} cX + \mu, & \alpha \neq 1, \\ cX + \frac{2}{\pi} \beta c \log(c) + \mu, & \alpha = 1. \end{cases} \quad (7)$$

Furthermore, we can generate the α -stable Lévy process by utilizing the above random number generation algorithm.

Probability density functions (PDFs) of $L(\zeta : \alpha, \beta, c, \mu)$ for various stability indexes and skewness parameters are illustrated in Fig. 5. As one can see, when skewness $\beta = 0$, the impulsiveness strengthens and the tail of the distribution becomes heavier as the stability index decreases. When $\alpha = 2$, it becomes a Gaussian distribution [see Fig. 5(a)]. Moreover, for fixed $\alpha = 1.5$, the augment in the absolute value of skewness leads to the more asymmetric distribution [see Fig. 5(b)]. When $\beta < 0$, the distribution is left-skewed and right-skewed for $\beta > 0$. The trajectories of the Lévy process and

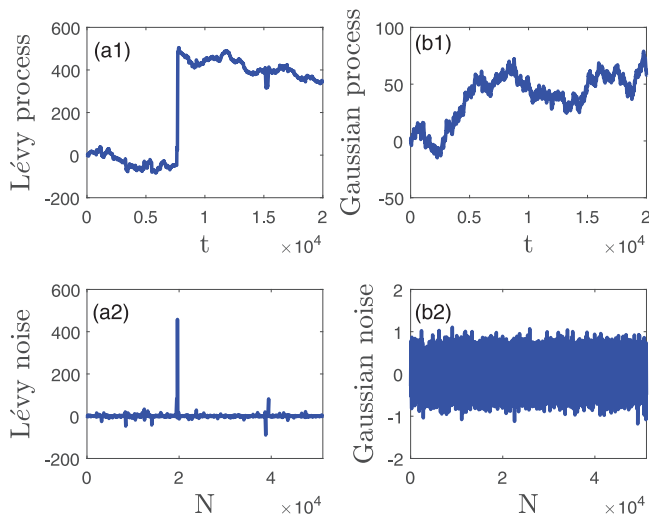


FIG. 6. (a) Lévy process and corresponding Lévy noise with $\alpha = 1.4$, $\beta = 0.2$, and $\sigma = 0.1$; (b) Gaussian process and corresponding Gaussian noise with $\alpha = 2$, $\beta = 0$, and $\sigma = 0.1$.

the corresponding Lévy noise are shown in Fig. 6. We can observe the distinct jumps when α is relatively small [see Fig. 6(a)]. However, the extreme jumps almost cannot occur when $\alpha = 2$, i.e., Gaussian noise [see Fig. 6(b)]. It is thus evident that the Lévy noise is

more suitable to characterize the pulsing changes of the stochastic environment driven by sudden climate events.

III. RESULTS

A. Switches induced by Lévy noise

The stationary probability density (SPD) is one of the key tools to explore the dynamical behaviors of a multistable model.^{34–36} In the bistable phosphorus dynamical model, noise can induce the phosphorus concentration in lake water to jump frequently between the two nutritional states (see Fig. 4); thus, the SPD of the phosphorus concentration may exhibit a bimodal distribution near the two stable equilibrium points. Statistically, the higher possession probability determines the final level of phosphorus concentration in lake water.

The Fokker-Planck equation (FPE) is an important deterministic tool for quantifying the stochastic differential equation. The equivalent FPE of model (2), which describes the evolution of the transition probability density for a stochastic system, has the following spatial fractional-order form:

$$\frac{\partial}{\partial t} u(P, t) = -\frac{\partial}{\partial P} [f(P)u(P, t)] + \frac{1 + \beta}{2} D(t)D_+^\alpha u(P, t) + \frac{1 - \beta}{2} D(t)D_-^\alpha u(P, t), \quad (8)$$

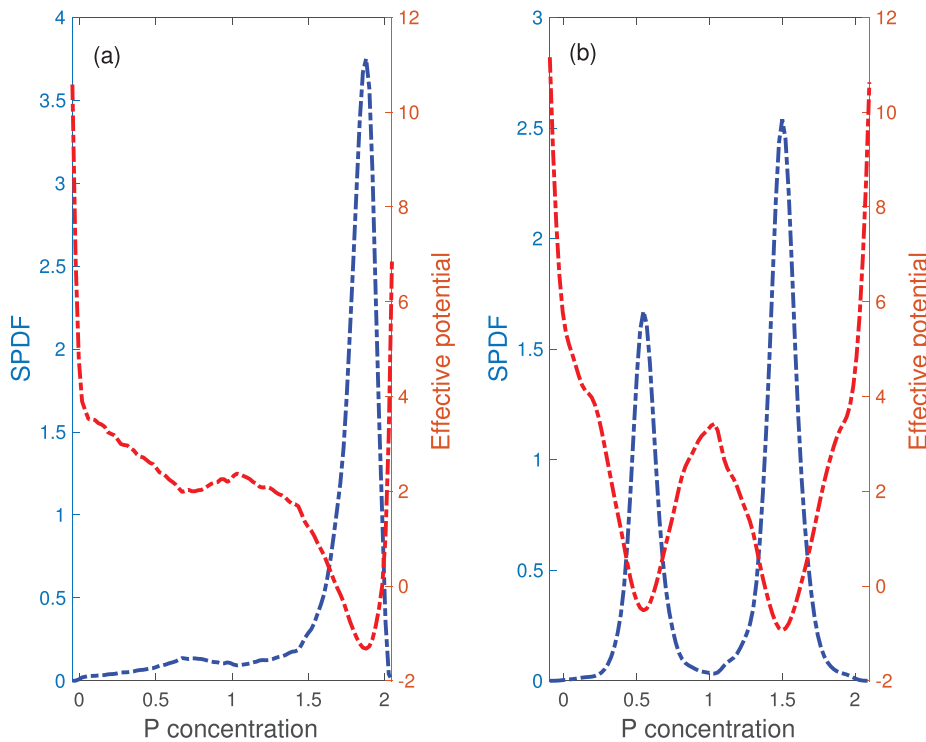


FIG. 7. SPDs of phosphorus concentration (blue dotted curve) and corresponding effective potential (red dotted curve) for different Lévy noise parameters: (a) $\alpha = 1.1$, $\beta = -0.7$, and $\sigma = 0.06$; (b) $\alpha = 1.5$, $\beta = 0.2$, and $\sigma = 0.02$.

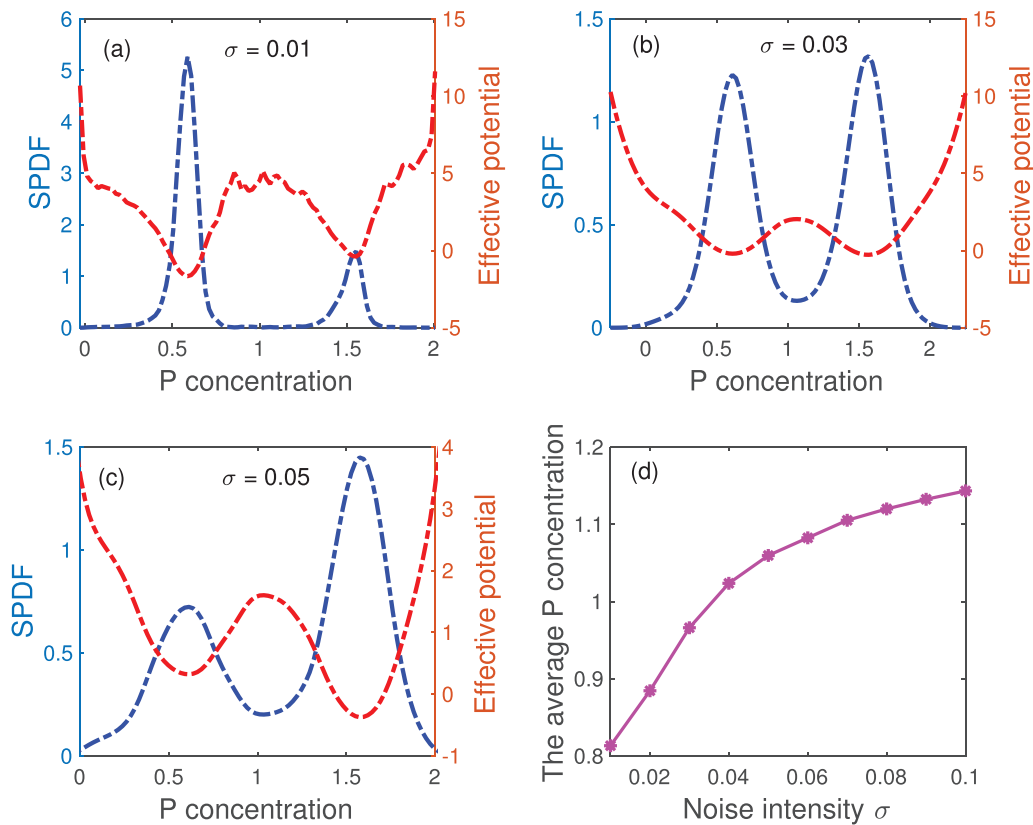


FIG. 8. The stationary probability density function (blue dotted curve) and corresponding effective potential (red dotted curve) with different noise intensities and fixed skewness $\beta = -0.6$ and stability index $\alpha = 1.5$: (a) $\sigma = 0.01$, (b) $\sigma = 0.03$, and (c) $\sigma = 0.05$. (d) The average phosphorus concentration vs σ .

where $f(P) = a - bP + \frac{rP^q}{m^q + P^q}$, $D(t)$ is the time-dependent coefficient of dispersion,

$$D_+^\alpha u(P, t) = \frac{1}{\Gamma(2 - \alpha)} \frac{\partial^2}{\partial P^2} \int_{L_1}^P \frac{u(\eta, t)}{(P - \eta)^{\alpha-1}} d\eta,$$

and

$$D_-^\alpha u(P, t) = \frac{1}{\Gamma(2 - \alpha)} \frac{\partial^2}{\partial P^2} \int_P^{L_2} \frac{u(\eta, t)}{(P - \eta)^{\alpha-1}} d\eta,$$

which represent the left and right Riemann–Liouville space fractional derivatives of order α for $u(P, t)$, $P \in [L_1, L_2]$ with L_1 and L_2 being the non-negative real numbers. In our paper, P denotes phosphorus concentration and then the interval is constrained to $[0, +\infty]$. In general, it is difficult to solve Eq. (8); thus, we only attempt to seek the numerical solution utilizing the fourth-order Runge–Kutta algorithm as follows:

$$P_{n+1} = P_n + \frac{1}{6}(k_1 + 2k_2 + 2k_3 + k_4) + \Delta t^{1/\alpha} \zeta_n, \quad (9)$$

where

$$\begin{cases} k_1 = \Delta t f(P_n), \\ k_2 = \Delta t f(P_n + k_1/2), \\ k_3 = \Delta t f(P_n + k_2/2), \\ k_4 = \Delta t f(P_n + k_3), \end{cases} \quad (10)$$

with $f(P_n) = a - bP_n + \frac{rP_n^q}{m^q + P_n^q}$, and ζ_n is the α -stable Lévy distributed random number in the n th time interval. In order to facilitate our discussion, all simulations in this paper are performed with the initial phosphorus concentration $P(0) = P_{S1} = 0.55$ and time step $\Delta t = 0.01$. Using Eqs. (9) and (10), we acquire the stationary probability density of phosphorus concentration.

Figure 7 shows the stationary probability density for different Lévy noise parameters. We observe that the altering of noise parameters can lead to the change of SPD from unimodal [see Fig. 7(a)] to bimodal [see Fig. 7(b)]. This implies that Lévy noise has a significant effect on the switching mechanism in the phosphorus dynamics. We will analyze the effects of Lévy noise on the switching dynamics of model (1) by utilizing the qualitative changes of the SPD and the MFPT.

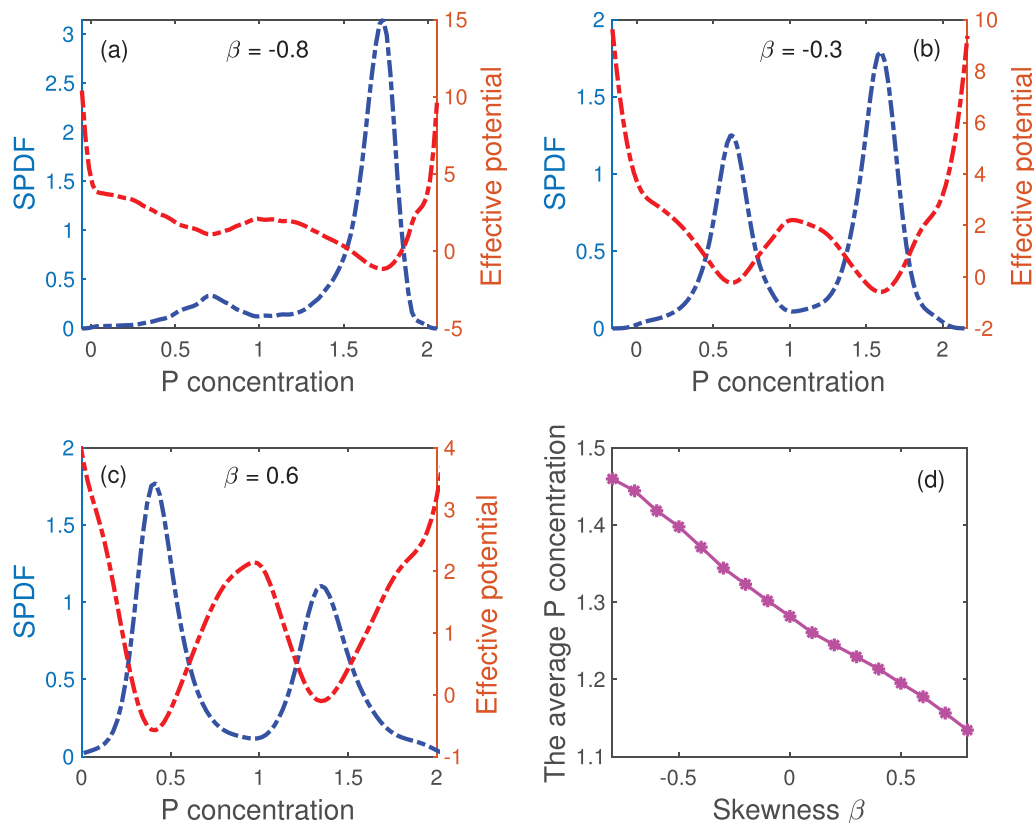


FIG. 9. The stationary probability density function (blue dotted curve) and corresponding effective potential (red dotted curve) with different skewness and fixed noise intensity $\sigma = 0.05$ and stability index $\alpha = 1.2$: (a) $\beta = -0.8$, (b) $\beta = -0.3$, and (c) $\beta = 0.6$. (d) The average phosphorus concentration vs. β .

Fixing skewness $\beta = -0.6$ and stability index $\alpha = 1.5$, we plot the SPDs of phosphorus concentration for different noise intensities in Fig. 8. The results show that when the noise intensity σ is at a smaller level ($\sigma = 0.01$), a curve of the probability density function has two peaks, and the peak near the lower equilibrium point is much higher, which indicates that the random orbit is mainly concentrated in the low-concentration state. In this case, the nutrient level of the lake is in an oligotrophic state. When the noise intensity increases further, the height change process of the two peaks is observed [see Figs. 8(b) and 8(c)]. The peak on the side of high phosphorus concentration becomes higher while the peak corresponding to low phosphorus concentration diminishes gradually. When σ exceeds the threshold value that the two peaks share the same heights, the state of high phosphorus concentration becomes more dominant, and thus we can say that the oligotrophic state to the eutrophic state switching occurs. This indicates that σ can induce positive feedback to boost phosphorus concentration in lake. According to the method in Ref. 37, we also depict the shape of the effective potential corresponding to the stationary probability density in Figs. 8(a)–8(c). Obviously, the phosphorus concentration evolves toward the local minimum of the effective potential, analogous to a ball rolling toward the bottom of a cup. In Fig. 8(d),

we exhibit the variation of the average phosphorus concentration \bar{P} with noise intensity σ . Here, $\bar{P} = \int_0^{+\infty} P \cdot u_{st}(P) dP$, where $u_{st}(P)$ is the stationary probability density function as time approaches infinity. It is clear that \bar{P} has the monotone increasing behavior with the increasing of σ . All the facts indicate that noise intensity σ promotes the transition from the oligotrophic state to the eutrophic state.

Next, we explore the impact of the skewness parameter β in the Lévy noise on the transition. In Fig. 9, we depict the SPDs of phosphorus concentration with three different values of skewness parameter and fix the noise intensity $\sigma = 0.05$ and stability index $\alpha = 1.2$. When the skewness is small ($\beta = -0.8$), the stationary occupation probability of the high phosphorus concentration state is larger than the lower state. As the skewness increases, the left peak of the SPD becomes higher gradually [see Fig. 9(b)]. When the skewness is quite large, the SPD achieves a total reversal in height. There is a high probability for a shift from the high phosphorus concentration state to the low state. This observation discloses that the skewness parameter can induce a transition from the eutrophic state to the oligotrophic state. A dependence of the mean values of phosphorus concentration on the skewness β is shown in Fig. 9(d). Under increasing skewness parameter, the mean value \bar{P} of phosphorus concentration monotone decreases. This result has a good

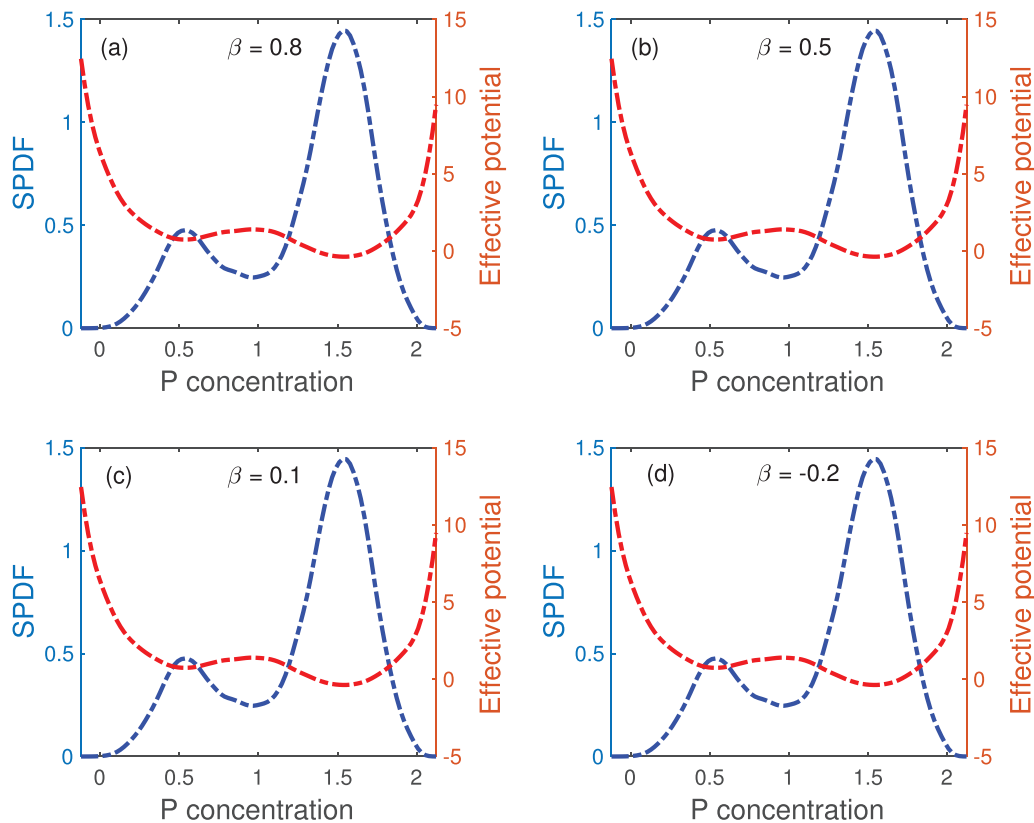


FIG. 10. The stationary probability density function (blue dotted curve) and corresponding effective potential (red dotted curve) with different skewness and fixed noise intensity $\sigma = 0.03$ and stability index $\alpha = 2$ (in the Gaussian case): (a) $\beta = 0.8$, (b) $\beta = 0.5$, (c) $\beta = 0.1$, and (d) $\beta = -0.2$.

agreement with the analyses above. However, when $\alpha = 2$, there are no distinct variations in the height and location of higher and lower peaks (see Fig. 10). In other words, in the Gaussian case, β loses its role and becomes dispensable. Compared with Fig. 8, we uncover in Fig. 9 that β significantly shifts the position of the two peaks. In fact, as we mentioned earlier, when $\beta > 0$ Lévy distribution is right-skewed, while for $\beta < 0$ it is left-skewed. When deterministic system (1) is disturbed by right-skewed ($\beta > 0$) Lévy noise, the noise will make phosphorus concentration smaller in the mean sense.

Finally, we explore the influence of the stability index α . Fixing $\sigma = 0.02$ and $\beta = -0.5$, by numerical simulation of model (2), the SPDFs of the phosphorus concentration are shown in Fig. 11. Initially, the stationary occupation probability at high phosphorus state is slightly higher than that at low phosphorus state. By strengthening the stability index, the peak height of the low phosphorus state increases and finally surpasses the other peak as the stability index exceeds a threshold [see Fig. 11(c)]. This process is analogous to the variations of skewness parameters (see Fig. 9). However, when the stability index reaches a certain value, the peak at the high phosphorus concentration state becomes more populated again

[see Fig. 11(d)]. Figure 12 shows the average phosphorus concentration vs α . Obviously, the behavior of the average phosphorus concentration does not change monotonically; instead, the \bar{P} first decreases, reaches a minimum at $\alpha = 1.5$, and then increases with increasing stability index for $\sigma = 0.02$ and $\beta = -0.5$. This conclusion is in agreement with the analyses of SPDFs. These results imply that the stability index can push the system to shift from high phosphorus concentration to low phosphorus concentration and vice versa. Meanwhile, we could find an optimal stability index to minimize the average phosphorus concentration when σ and β are fixed.

B. Mean first passage time

An extensive number of studies disclose that the eutrophication of freshwater and coastal marine ecosystems depends on the nutrient levels,^{38–40} and how fast the transition between different nutrient levels occur directly reflects the sensitivity of the ecosystem to the variation of the environmental conditions. Therefore, it is necessary to investigate the switching timing of the phosphorus concentration at the oligotrophic state crossing the unstable equilibrium state

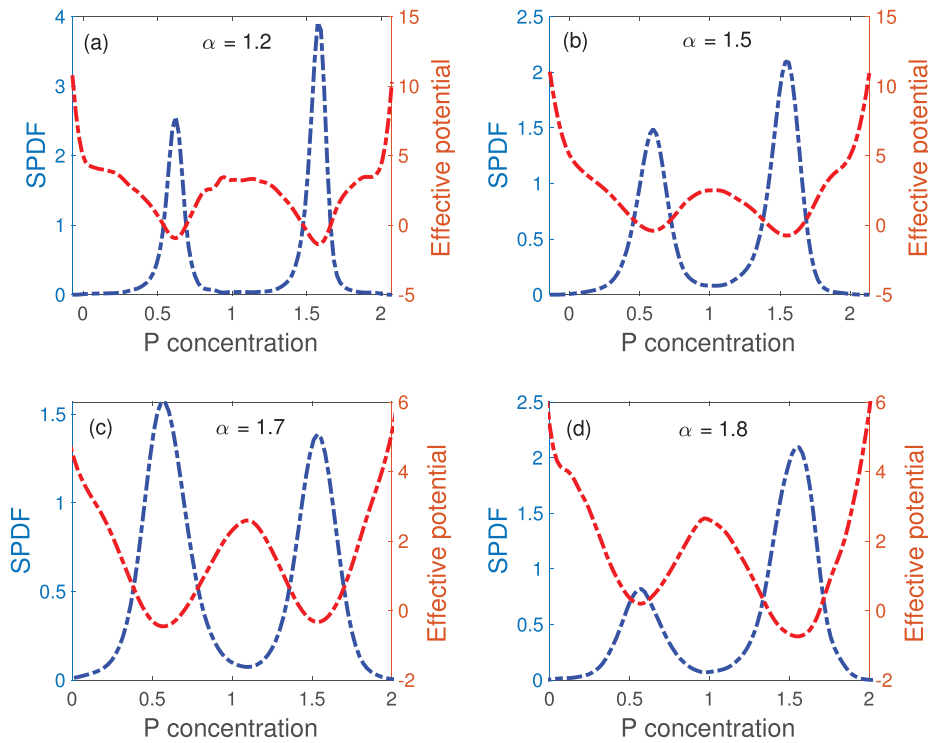


FIG. 11. The stationary probability density function (blue dotted curve) and corresponding effective potential (red dotted curve) with different stability indices and fixed noise intensity $\sigma = 0.02$ and skewness $\beta = -0.5$: (a) $\alpha = 1.2$, (b) $\alpha = 1.5$, (c) $\alpha = 1.7$, and (d) $\alpha = 1.8$.

to the eutrophic state. In general, this switching time is called the first passage time (FPT), which is defined as the time taken for a random trajectory to reach another regime for the first time.³¹ The statistical average of FPT is referred to as the mean first passage time (MFPT). Unlike the SPDs discussed in Sec. III A, which describe the

steady-state characteristics of the system, the mean first passage time is one of the most suitable methods to capture the switching dynamics of phosphorus concentration. Recently, Padash *et al.*^{41,42} have given explicit analytical results of MFPT in certain special cases. In this section, however, we will numerically calculate MFPT to discuss the effect of Lévy noise on the switching behaviors of phosphorus concentration. For lake managers, it is meaningful to monitor the nutrient status of lakes and prevent them from becoming worse. Therefore, here we only calculate the MFPT of model (2) from the oligotrophic state to the eutrophic state. The initial value is set as $P(0) = P_{S1}$, and we define the FPT as

$$\tau = \inf \{t : P(t) > P_{S2}\}. \tag{11}$$

Taking an average on the FPT generates the MFPT,

$$MFPT = E[\tau]. \tag{12}$$

Applying the Monte Carlo method for the numerical simulation, if $P(k\Delta t) > P_{S2}$, then $\tau = k\Delta t$. Let the number of simulation times be N , then

$$MFPT = \frac{\sum_{j=0}^N k_j \Delta t}{N}. \tag{13}$$

Here, we take $N = 1000$.

Figure 13 presents the MFPT vs σ , β , and α . In Fig. 13(a), it is obvious that the MFPT decreases with the increases of σ . In other words, when the initial phosphorus concentration is at the low level, as the environmental disturbance gets stronger, the transition from state P_{S1} to state P_{S2} becomes easier, and this declares that the noise

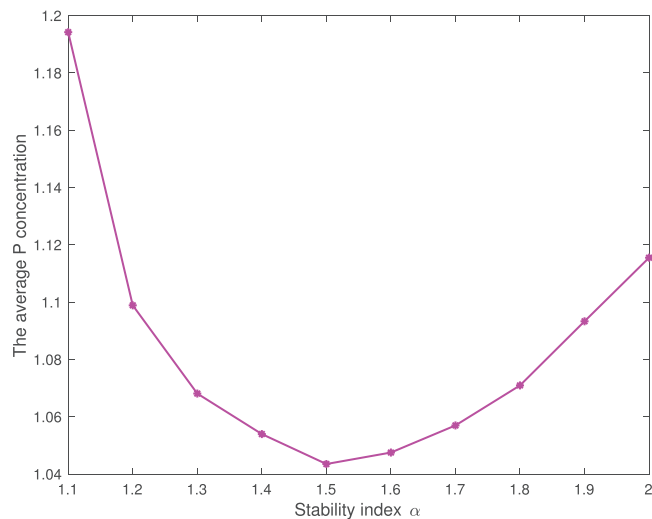


FIG. 12. The average phosphorus concentration vs α .

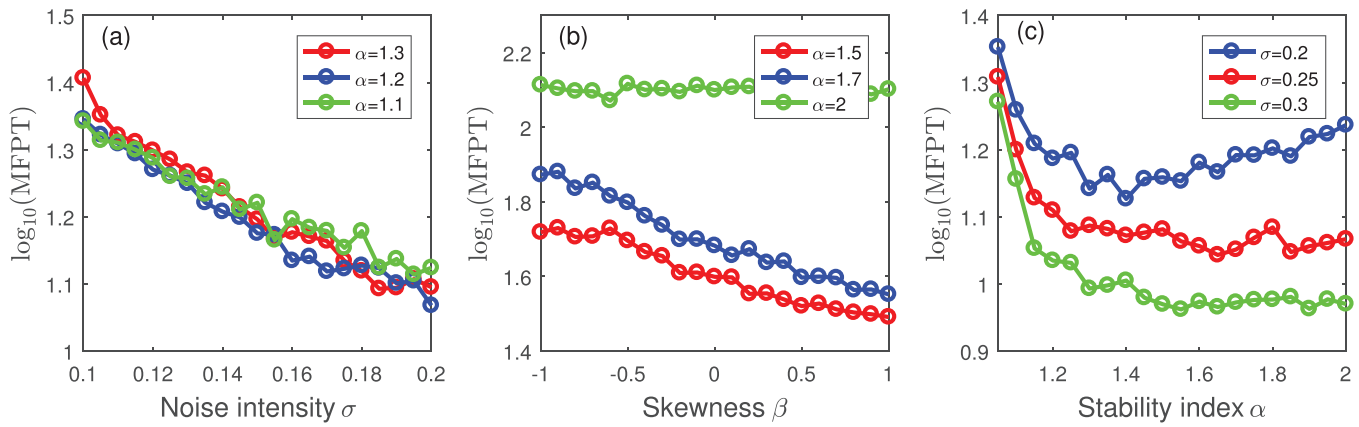


FIG. 13. MFPT of phosphorus concentration transferring from the low phosphorus equilibrium state P_{S1} to the high phosphorus equilibrium state P_{S2} . (a) The MFPT vs noise intensity ($\beta = 0.1$); (b) the MFPT vs skewness ($\sigma = 0.1$); and (c) the MFPT vs stability index ($\beta = 0.5$). The simulated results are generated by averaging $N = 1000$ realizations.

intensity may accelerate lake eutrophication. In ecology, one can deduce that the algal blooms will occur at earlier times for larger environmental fluctuations. Next, we discuss the influence of the skewness parameter on MFPT. Figure 13(b) shows how the MFPT varies with the skewness parameter β for different stability indices $\alpha = 1.5$, $\alpha = 1.7$, and $\alpha = 2$. The transition process becomes easier with the decrease of the stability index α and the increase of the skewness parameter β . It suggests that a small stability index and a large skewness parameter can speed up lake eutrophication. In addition, in the case of Gaussian ($\alpha = 2$), the skewness parameter has little impact on the switching time. The relationship between α and MFPT for different noise intensities σ is shown in Fig. 13(c). MFPT shows a decreasing trend as α increases. For a relatively strong noise

intensity, after α exceeds a critical value, MFPT is insensitive to changes in α . In stochastic model (2), the noise intensity σ and the stability index α can be considered as the intensity and the frequency of extreme weather events. Therefore, Fig. 13(c) illustrates that the increased intensity and frequency of extreme climate events have a positive effect on lake eutrophication, but when the frequency exceeds a critical value, the intensity of extreme events becomes the most key culprit for lake eutrophication.

C. Real data analysis

In this section, we will quantify the linkage among extreme monthly precipitation, chlorophyll-a concentration, and P

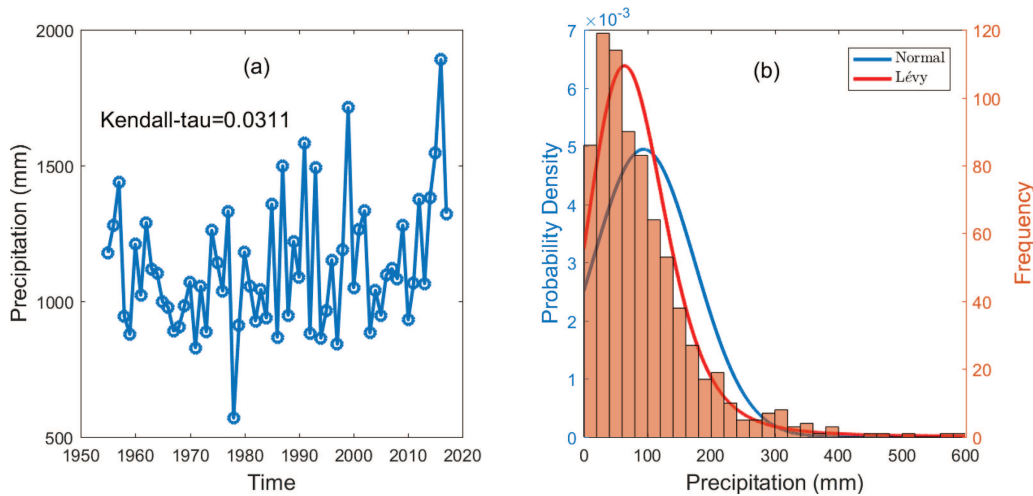


FIG. 14. (a) Annual precipitation from 1955 to 2017 (data are from the Wuxi Meteorological Station); (b) probability density function of monthly precipitation fitted by Lévy (red curve) and normal (blue curve) distributions.

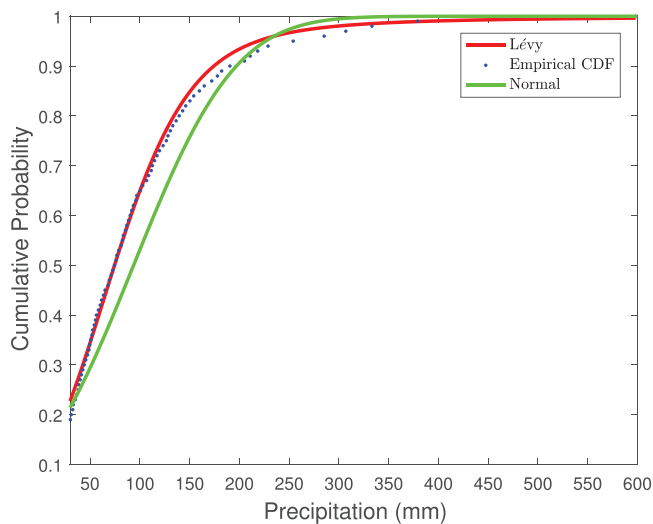


FIG. 15. Cumulative probabilities of Lévy distribution and normal distribution fitting by McCulloch's method⁴⁴ to the monthly precipitation data from 1955 to 2017.

concentration for Lake Taihu, China, using the Lévy-stable distribution. Real data used in this article are collected in Ref. 43. In Fig. 14(a), the annual rainfall in the Lake Taihu area shows an increasing trend since 1955 (Kendall- $\tau = 0.0311$) and reaches the

highest value in 2016. We fit the Lévy distributions and the normal distributions to the monthly precipitation data [Fig. 14(b)] and compare the tails of the cumulative distributions (Fig. 15). Here, we use the quantile method proposed by McCulloch⁴⁴ to estimate the four parameters of the stable distribution. Obviously, the fit of the Lévy distribution is much better than that of the normal distribution. The tail of the Lévy distribution extends to greater rainfall levels than the tail of the normal distribution. Parameters of the best-fitting Lévy distribution are $\hat{\alpha} = 1.71658$, $\hat{\beta} = 1$, $\hat{c} = 44.0314$, and $\hat{\mu} = 88.1762$. The stability index $\hat{\alpha} < 2$ indicates that monthly rainfall has a thicker tail than the normal distribution. Figure 16 shows the time series of P load (kt), monthly mean phosphorus concentration (mg/l), and monthly mean Chl-a concentration (g/l) in Lake Taihu from 2014 to 2018. Flooding in the Taihu Lake basin in June 2016 resulted in higher external phosphorus input, and chlorophyll-a and phosphorus concentrations increased rapidly in July of the same year (green shadows in Fig. 16). For P concentration and Chl-a concentration of Lake Taihu, the results of fitting the Lévy and normal distribution are shown in Fig. 17. The Lévy distribution is more suitable for fitting data with heavy tails, and the best fitting parameters are $\hat{\alpha}_1 = 1.70391$, $\hat{\beta}_1 = 1$, $\hat{c}_1 = 0.0323826$, $\hat{\mu}_1 = 0.149993$, and $\hat{\alpha}_2 = 2$, $\hat{\beta}_2 = 1$, $\hat{c}_2 = 34.6381$, and $\hat{\mu}_2 = 31.7413$.

In order to explore the impact of extreme rainfall events on P and Chl-a concentrations in Lake Taihu, we divide the time series data of P and Chl-a concentrations into two parts, 12 months (from 2015-6 to 2016-5) before and 12 months (from 2016-7 to 2017-6) after extreme rainfall (2016-6), and use Lévy distribution to fit these

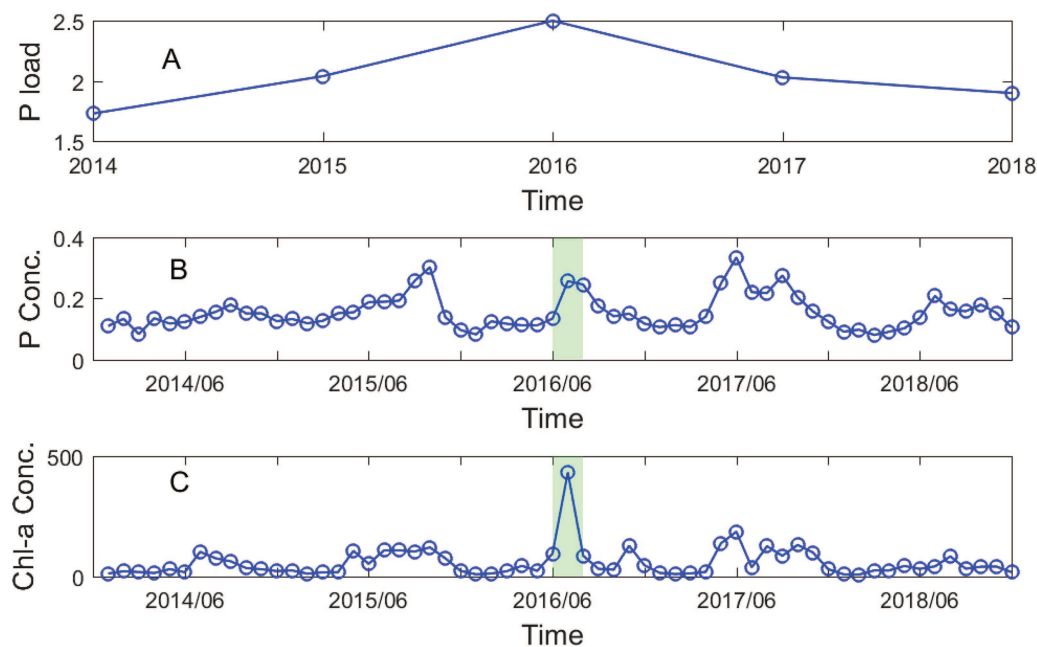


FIG. 16. Time series of (a) annual riverine P load (kt), (b) monthly mean P concentration (mg/l), and (c) monthly mean Chl-a concentration ($\mu\text{g/l}$) in Lake Taihu from 2014 to 2018.

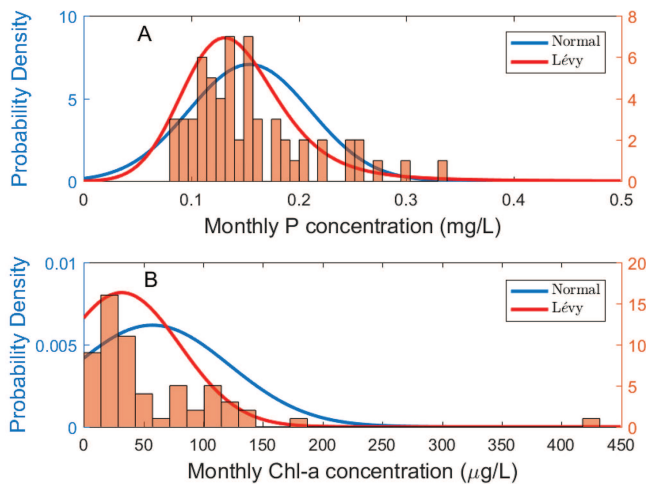


FIG. 17. Probability density functions of (a) monthly phosphorus and (b) chlorophyll-a concentrations are fitted by Lévy (red curve) and normal (blue curve) distributions.

data. The stability index α of Chl-a concentration decreases after heavy rainfall. Therefore, the tail of distribution for Chl-a concentration after heavy rainfall is thicker than that before heavy rainfall [Fig. 18(a)]. The scale parameter c of P and Chl-a concentrations both increase after heavy rainfall [Figs. 18(a) and 18(b)], indicating that heavy rainfall has a strong impact on extreme values of P and Chl-a concentrations.

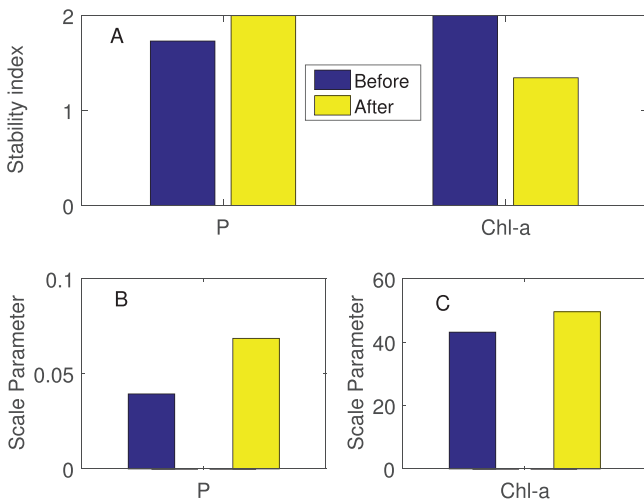


FIG. 18. Parameters of the Lévy distribution for P and Chl-a concentrations in Lake Taihu before and after extreme precipitation events. (a) Stability index α . (b) and (c) scale parameter c .

IV. CONCLUSIONS

Abrupt changes (regime shifts) in ecological systems refer to the state of a system suddenly changing from its current state to a completely different state (such as the shift from the oligotrophic state to the eutrophic state in a studied lake) when external drivers exceed a tipping point. These regime shifts usually involve the slow change of parameters of a system and the interference of sudden stochastic events such as hurricanes and heavy precipitation events. A growing number of empirical studies suggest that climate extremes can force abrupt ecological changes. For example, Carpenter *et al.*¹¹ studied Lake Mendota, located in southern Wisconsin, and found that the trend toward more frequent and intense precipitation extremes will increase phosphorus loading and intensify the eutrophication of the lake. Motew *et al.*⁴⁵ obtained a similar conclusion. Moreover, Carpenter *et al.* observed the phycocyanin concentration of Lake Mendota during the ice-free seasons from 2008 to 2018 through sensors, indicating that environmental stochasticity can drive the sudden changes of phycocyanin concentration between high and low states.^{7,46} It is worthy to remark that environmental stochasticity in Refs. 7 and 46 was characterized by Gaussian white noise instead of non-Gaussian Lévy noise.

It is predicted that the frequency and intensity of extreme weather events will continue to increase in the near future,⁴⁷ which will intensify biological, chemical, and physical disturbances in shallow lakes.¹² For a realistic ecosystem model, the idealized hypothesis about the Gaussianity of environmental noise is unrealistic. In fact, by collecting and analyzing decades-long time series data from 11 lakes, Batt *et al.*⁴⁸ found that data of meteorological variables (e.g., rainfall), data of chemical variables (e.g., nutrients, pH), and data of biological variables (e.g., population size) are mostly heavy-tailed distributions. Hence, in order to gain insights into the phosphorus concentration variations in lakes disturbed by extreme weather conditions, we proposed a parameterized lake eutrophication model under the non-Gaussian α -stable Lévy noise.

First, we obtained the stationary probability density function of model (2) based on the CMS algorithm and examined the effects of Lévy noise parameters (noise intensity, skewness parameter, and stability index) on the qualitative changes of SPD of phosphorus concentration. The results show that the noise-induced switch is significantly different for non-Gaussian α -stable Lévy noise compared with the Gaussian white noise. In addition to noise intensity, skewness parameter and stability index both play pivotal roles in the switching behavior of phosphorus concentration.

Next, we quantified the impact of non-Gaussian Lévy noise on the MFPT for phosphorus concentration to switch from initial value $P(0) = P_{S1}$ (the low phosphorus state) to the high phosphorus state P_{S2} . Numerical results show that σ , β , and α accelerate the transition of phosphorus in the water column from the low-concentration state to the high-concentration state, which means that Lévy noise parameters can facilitate the eutrophication of lakes by reducing the switching time. We also find that β becomes inessential and has no impact on the MFPT when $\alpha = 2$ in the Gaussian case.

Finally, we applied the Lévy distribution to analyze the extremes of precipitation, P concentration, and Chl-a concentration. Our result shows that extreme rainfall is closely related to extreme P and Chlorophyll-a concentrations. Therefore, during and after

extreme rainfall events, reducing phosphorus runoff and transport by policymakers is a key initiative to mitigate eutrophication.

As a summary, in order to understand the mechanism of abrupt changes in lake nutrient levels affected by extreme climate events, we proposed a new research method, based on the α -stable Lévy distribution, to reveal the dependence of lake nutrient levels on the intensity and frequency of extreme climate noise. Compared with the work in Refs. 11 and 48, we not only used traditional statistical methods to analyze the impact of extreme weather on lake nutrient levels based on actual data but also employed dynamic tools to explore the role of key noise parameters. However, we only considered a univariate model in this article. It is well known that P is a necessary nutrient to promote the growth of algae. Therefore, mathematical models used to analyze lake eutrophication and algae outbreak normally consist of at least two variables: phosphorus and algae. Our novel method here is the first step to mechanistically model catastrophic weather events and will be extended to a phosphorus–algae model or even with herbivores in the near future. Furthermore, real ecosystems often involve three “tipping” mechanisms: bifurcation-induced tipping, rate-induced tipping, and noise-induced tipping. Our work belongs to the noise-induced tipping and has great potential to be applied in many different scenarios. For bifurcation-induced tipping, near a bifurcation point, the resilience of the system decreases. In other words, the disturbed system will take more time to recover to its stable state. This property is called “critical slowing down (CSD).” Recent research efforts aim to establish a set of suitable early warning signals (EWS) based on CSD, such as variance and autocorrelation, which can help prevent adverse events such as ecosystem collapse due to environmental changes. We will study EWS for predicting and preventing severe algae blooms in lake ecosystems.

ACKNOWLEDGMENTS

S.Y. gratefully acknowledges support from the National Natural Science Foundation of China (Nos. 12071293 and 11671260). H.W. gratefully acknowledges support from the Natural Sciences and Engineering Research Council of Canada (Discovery Grant No. RGPIN-2020-03911 and Accelerator Grant No. RGPAS-2020-00090).

AUTHOR DECLARATIONS

Conflict of Interest

The authors have no conflicts to disclose.

Author Contributions

All authors contributed equally to this work.

DATA AVAILABILITY

The data that support the findings of this study are available within the article.

REFERENCES

- ¹B. Qin, P. Xu, Q. Wu, L. Luo, and Y. Zhang, “Environmental issues of Lake Taihu, China,” in *Eutrophication of Shallow Lakes with Special Reference to Lake Taihu, China* (Springer, 2007), pp. 3–14.
- ²B. Qin, G. Zhu, G. Gao, Y. Zhang, W. Li, H. W. Paerl, and W. W. Carmichael, “A drinking water crisis in Lake Taihu, China: Linkage to climatic variability and lake management,” *Environ. Manage.* **45**(1), 105–112 (2010).
- ³L. Guo, “Doing battle with the green monster of Taihu Lake,” *Science* **317**(5842), 1166 (2007).
- ⁴H. Xu, H. Paerl, B. Qin, G. Zhu, N. Hall, and Y. Wu, “Determining critical nutrient thresholds needed to control harmful cyanobacterial blooms in eutrophic Lake Taihu, China,” *Environ. Sci. Technol.* **49**(2), 1051–1059 (2015).
- ⁵S. R. Carpenter, *Regime Shifts in Lake Ecosystems: Pattern and Variation*, Excellence in Ecology Series 15 (University of Wisconsin-Madison, 2003).
- ⁶D. Ludwig, S. Carpenter, and W. Brock, “Optimal phosphorus loading for a potentially eutrophic lake,” *Ecol. Appl.* **13**(4), 1135–1152 (2003).
- ⁷S. R. Carpenter, B. M. Arani, P. C. Hanson, M. Scheffer, E. H. Stanley, and E. Van Nes, “Stochastic dynamics of cyanobacteria in long-term high-frequency observations of a eutrophic lake,” *Limnol. Oceanogr. Lett.* **5**(5), 331–336 (2020).
- ⁸Y. Zhang, B. Qin, G. Zhu, G. Gao, L. Luo, and W. Chen, “Effect of sediment resuspension on underwater light field in shallow lakes in the middle and lower reaches of the Yangtze River: A case study in Longgan Lake and Taihu Lake,” *Sci. China Ser. D* **49**(1), 114–125 (2006).
- ⁹M. Søndergaard, P. Kristensen, and E. Jeppesen, “Phosphorus release from resuspended sediment in the shallow and wind-exposed lake Arresø, Denmark,” *Hydrobiologia* **228**(1), 91–99 (1992).
- ¹⁰S. R. Carpenter, “Eutrophication of aquatic ecosystems: Bistability and soil phosphorus,” *Proc. Natl. Acad. Sci. U.S.A.* **102**(29), 10002–10005 (2005).
- ¹¹S. R. Carpenter, E. G. Booth, and C. J. Kucharik, “Extreme precipitation and phosphorus loads from two agricultural watersheds,” *Limnol. Oceanogr.* **63**(3), 1221–1233 (2018).
- ¹²M. L. Fogel, C. Aguilar, R. Cuhel, D. J. Hollander, J. D. Willey, and H. W. Paerl, “Biological and isotopic changes in coastal waters induced by Hurricane Gordon,” *Limnol. Oceanogr.* **44**(6), 1359–1369 (1999).
- ¹³M. Zhu, H. W. Paerl, G. Zhu, T. Wu, W. Li, K. Shi, L. Zhao, Y. Zhang, B. Qin, and A. M. Caruso, “The role of tropical cyclones in stimulating cyanobacterial (*Microcystis* spp.) blooms in hypertrophic Lake Taihu, China,” *Harmful Algae* **39**, 310–321 (2014).
- ¹⁴J. Ma, Y. Xu, W. Xu, Y. Li, and J. Kurths, “Slowing down critical transitions via Gaussian white noise and periodic force,” *Sci. China Technol. Sci.* **62**(12), 2144–2152 (2019).
- ¹⁵J. Ma, Y. Xu, Y. Li, R. Tian, and J. Kurths, “Predicting noise-induced critical transitions in bistable systems,” *Chaos* **29**(8), 081102 (2019).
- ¹⁶S. R. Carpenter and W. A. Brock, “Rising variance: A leading indicator of ecological transition,” *Ecol. Lett.* **9**(3), 311–318 (2006).
- ¹⁷L. Defew, L. May, and K. Heal, “Uncertainties in estimated phosphorus loads as a function of different sampling frequencies and common calculation methods,” *Mar. Freshwater Res.* **64**(5), 373–386 (2013).
- ¹⁸A. La Cognata, D. Valenti, A. Dubkov, and B. Spagnolo, “Dynamics of two competing species in the presence of Lévy noise sources,” *Phys. Rev. E* **82**(1), 011121 (2010).
- ¹⁹H. Zhang, W. Xu, Y. Lei, and Y. Qiao, “Noise-induced vegetation transitions in the grazing ecosystem,” *Appl. Math. Model.* **76**, 225–237 (2019).
- ²⁰A. V. Chechkin, V. Y. Gonchar, J. Klafter, and R. Metzler, “Barrier crossing of a Lévy flight,” *Europhys. Lett.* **72**, 348 (2005).
- ²¹A. V. Chechkin, O. Y. Sliusarenko, R. Metzler, and J. Klafter, “Barrier crossing driven by Lévy noise: Universality and the role of noise intensity,” *Phys. Rev. E* **75**, 041101 (2007).
- ²²P. Ditlevsen, “Anomalous jumping in a double-well potential,” *Phys. Rev. E* **60**, 172 (1999).
- ²³P. Imkeller and I. Pavlyukevich, “First exit times of SDES driven by stable Lévy processes,” *Stoch. Proc. Appl.* **116**, 611–642 (2006).
- ²⁴P. Imkeller and I. Pavlyukevich, “Lévy flights: Transitions and meta-stability,” *J. Phys. A: Math. Gen.* **39**, L237 (2006).
- ²⁵Y. Xu, J. Li, J. Feng, H. Zhang, W. Xu, and J. Duan, “Lévy noise-induced stochastic resonance in a bistable system,” *Eur. Phys. J. B* **86**(5), 1–7 (2013).

- ²⁶B. Dybiec and E. Gudowska-Nowak, "Lévy stable noise-induced transitions: Stochastic resonance, resonant activation and dynamic hysteresis," *J. Stat. Mech. Theory Exp.* **2009**(05), P05004 (2009).
- ²⁷A. Yang, B. Song, and S. Yuan, "Noise-induced transitions in a non-smooth SIS epidemic model with media alert," *Math. Biosci. Eng.* **18**(1), 745–763 (2021).
- ²⁸J. Gao, S. Hwang, and J. Liu, "When can noise induce chaos?," *Phys. Rev. E* **82**(6), 1132 (1999).
- ²⁹S. R. Carpenter, D. Ludwig, and W. A. Brock, "Management of eutrophication for lakes subject to potentially irreversible change," *Ecol. Appl.* **9**(3), 751–771 (1999).
- ³⁰R. Wang, J. A. Dearing, P. G. Langdon, E. Zhang, X. Yang, V. Dakos, and M. Scheffer, "Flickering gives early warning signals of a critical transition to a eutrophic lake state," *Nature* **492**(7429), 419–422 (2012).
- ³¹J. Duan, *An Introduction to Stochastic Dynamics* (Cambridge University Press, 2015), Vol. 51.
- ³²A. Weron and R. Weron, "Computer simulation of Lévy α -stable variables and processes," in *Chaos—The Interplay Between Stochastic and Deterministic Behaviour* (Springer, 1995), pp. 379–392.
- ³³R. Weron, "On the Chambers-Mallows-Stuck method for simulating skewed stable random variables," *Stat. Probab. Lett.* **28**(2), 165–171 (1996).
- ³⁴Y. Xu, Y. Li, H. Zhang, X. Li, and J. Kurths, "The switch in a genetic toggle system with Lévy noise," *Sci. Rep.* **6**(1), 1–11 (2016).
- ³⁵X. Chen, Y.-M. Kang, and Y.-X. Fu, "Switches in a genetic regulatory system under multiplicative non-Gaussian noise," *J. Theor. Biol.* **435**, 134–144 (2017).
- ³⁶Z. Huang, Q. Yang, and J. Cao, "Stochastic stability and bifurcation for the chronic state in Marchuk's model with noise," *Appl. Math. Model.* **35**(12), 5842–5855 (2011).
- ³⁷D. Bartłomiej, G.-N. Ewa, and S. IM, "Stationary states in Langevin dynamics under asymmetric Lévy noises," *Phys. Rev. E* **76**, 041122 (2007).
- ³⁸A. M. Michalak, E. J. Anderson, D. Beletsky, S. Boland, N. S. Bosch, T. B. Bridgeman, J. D. Chaffin, K. Cho, R. Confesor, I. Daloğlu *et al.*, "Record-setting algal bloom in Lake Erie caused by agricultural and meteorological trends consistent with expected future conditions," *Proc. Natl. Acad. Sci. U.S.A.* **110**(16), 6448–6452 (2013).
- ³⁹J. C. Ho and A. M. Michalak, "Phytoplankton blooms in Lake Erie impacted by both long-term and springtime phosphorus loading," *J. Great Lakes Res.* **43**(3), 221–228 (2017).
- ⁴⁰D. L. Correll, "The role of phosphorus in the eutrophication of receiving waters: A review," *J. Environ. Qual.* **27**(2), 261–266 (1998).
- ⁴¹A. Padash, A. V. Chechkin, B. Dybiec, M. Magdziarz, B. Shokri, and R. Metzler, "First passage time moments of asymmetric Lévy flights," *J. Phys. A: Math. Theor.* **53**, 275002 (2020).
- ⁴²A. Padash, A. V. Chechkin, B. Dybiec, I. Pavlyukevich, B. Shokri, and R. Metzler, "First-passage properties of asymmetric Lévy flights," *J. Phys. A: Math. Theor.* **52**, 454004 (2019).
- ⁴³B. Qin, J. Deng, K. Shi, J. Wang, J. Brookes, J. Zhou, Y. Zhang, G. Zhu, H. W. Paerl, and L. Wu, "Extreme climate anomalies enhancing cyanobacterial blooms in eutrophic Lake Taihu, China," *Water Resour. Res.* **57**(7), e2020WR029371 (2021).
- ⁴⁴J. H. McCulloch, "Simple consistent estimators of stable distribution parameters," *Commun. Stat. Simul. Comput.* **15**(4), 1109–1136 (1986).
- ⁴⁵M. Motew, E. G. Booth, S. R. Carpenter, X. Chen, and C. J. Kucharik, "The synergistic effect of manure supply and extreme precipitation on surface water quality," *Environ. Res. Lett.* **13**(4), 044016 (2018).
- ⁴⁶S. R. Carpenter, B. M. Arani, E. H. Van Nes, M. Scheffer, and M. L. Pace, "Resilience of phytoplankton dynamics to trophic cascades and nutrient enrichment," *Limnol. Oceanogr.* **67**, S258 (2021).
- ⁴⁷J. B. Elsner, J. P. Kossin, and T. H. Jagger, "The increasing intensity of the strongest tropical cyclones," *Nature* **455**(7209), 92–95 (2008).
- ⁴⁸R. D. Batt, S. R. Carpenter, and A. R. Ives, "Extreme events in lake ecosystem time series," *Limnol. Oceanogr. Lett.* **2**(3), 63–69 (2017).